Nature Environment and Pollution Technology
An International Quarterly Scientific Journal

p-ISSN: 0972-6268
(Print copies up to 2016)
e-ISSN: 2395-3454

Vol. 22 | No. 4 | pp. 1911-1920 | 2023

Original Research Paper

https://doi.org/10.46488/NEPT.2023.v22i04.017

Open Access Journal

Predictability Augmentation by In-silico Study to In-vivo and In-vitro Results of Lung Doses of Airborne Fine and Ultrafine Particles Inhaled by Humans at Industrial Workplaces

M. Ali†

Biosimulation and Aerosol Research Lab, Longview University Center, The University of Texas at Tyler, 3201 N. Eastman Road, Longview 75605, USA

†Corresponding author: M. Ali; mohammedali@uttyler.edu

Nat. Env. & Poll. Tech.
Website: www.neptjournal.com

Received: 04-04-2023
Revised: 07-06-2023
Accepted: 18-06-2023

Key Words:
Ultrafine particles
Carbon black
Lung deposition
Electrical discharge machining
MPPD model
Workplace pollution

ABSTRACT

This study correlates computational predictions with in vivo and in vitro experimental results of inhaled fine and ultrafine particulate matter (PM) transport, dissemination, and deposition in the human respiratory airways. Epidemiological studies suggest that workplace exposure to anthropogenic pollutant PMs is a risk factor for increased susceptibility to acute broncho-pulmonary illnesses. However, investigations on detailed human inhalation and PM transport processes are restrictive from time, cost, and ethical perspectives. Computational simulation based on the Multiple Path Particle Dosimetry (MPPD) model was employed to quantify the risks associated with workplace exposure of these PMs. Here, the physical, mechanical, and electrical properties of PMs of carbon black (CB) and ultrafine particles (UFPs) from wire-cut electrical discharge machining (WEDM), with mass median aerodynamic diameter (CMAD) in the range of 1 nm to 1000 nm, were used as input parameters of MPPD. Additionally, it mimicked occupational workers' age, body mass index, and oronasal-combinational nose and mouth breathing exposure time. The deposition results were compared with several vivo and in vitro experimental data reported in the literature, and satisfactory agreements were found. For example, a total lung dose of CB-PMs of 100 nm is the highest (28%), while a 380 nm dose is the lowest (15%). Afterward, deposition increases with particle size, reaching 26% for 1000 nm. In the case of WEDM-UFPs, about 98% of all 1.0 nm inhaled particles remain in the lung. Subsequently, the deposition dose decreases with the particle size and reaches up to 28% for 100 nm particles. Approximately 51% of deposited WEDM-UFPs are of CMAD ≤ 5 nm. The images of lung geometry also observed the maximum deposited mass and mass flux rate in the head, tracheobronchial, and pulmonary airways.

INTRODUCTION

It is a well-established concept that the human respiratory system represents a complicated air route with a defined structure-activity relationship. It is divided mainly into two regions: the conductive and respiratory regions. The conductive region comprises the nasal cavity, sinuses, nasopharynx, oropharynx, and larynx (combinedly "Head" airway), then the trachea, bronchi, and up to the terminal bronchioles (combinedly "TB" airway). The respiratory region comprises bronchioles, alveolar ducts, and alveolar sacs (combined "P" airway). The main functions of the conductive part are to filter, humidify, and warm the inhaled air, while the respiratory part functions as the place for oxygen and carbon dioxide gas exchanges (Douafera et al. 2020). However, the inhaled air and particulate matter (PMs), if carried along with it, will form an aerosol by mixing with airways' moisture. Fine particles are airborne smaller particles with an aerodynamic diameter (d_{ae}) of 2500 nm or less. The larger PMs (dia. > 2500 nm) deposit mostly in the conductive region, and the smaller ones will travel further into the respiratory region to cause systemic effects (either desirable or adverse).

Ultrafine particles (UFPs) are considered to have a d_{ae} < 100 nm or 0.1 micrometer. The human eye can see debris and dust approximately 25 microns in size. The PM_{10}, $PM_{2.5,}$ and UFPs are too small to be seen by the naked eye. More important, the origin and geometric size of PMs (100 nm ≤ d_{ae} ≤ 100 μm) permit them to hold a diversity of physicochemical, electromechanical, and biological (PEB) properties. However, when PM enters the lung airways, their size, surface areas, and PEB properties play a major role in interacting materials with biological systems. Among

them, the medicinal particles provide expected desirable therapy effects, and the pollutant or carcinogen particles provide unexpected adverse effects or diseases. To our knowledge, the lung burden refers to the quantity of retained material within the lungs, which is a function of pulmonary deposition and retention of inhaled nanoparticles, and this PM deposition causes unexpected adverse effects or diseases (Seong Jo et al. 2020, Abraham et al. 2002).

Engineered UFPs are purposefully developed in many applications (e.g., carbon black, fumed silica, titanium dioxide [TiO2], iron oxide [FeOx], quantum dots, and carbon nanotubes (Ali 2014, Matsoukas et al. 2015). High-energy processes such as synthesis, spraying, machining, and industrial bagging are correlated with the release of large numbers of predominantly fine particles and UFPs. The wide application of engineered UFPs has induced increasing exposure to humans and the environment, which has led to substantial concerns about their biosafety. In an extensive review of the production of engineered particles, Ding et al. (2017) showed that process-based release potential can be ranked and tied with exposure assessment approaches, which can guide the implementation of workplace safety measures. Their study also suggested that significant exposures largely occur at industrial workplaces when industrial safeguards and personal protection schemes are not followed as recommended.

Major concerns exist regarding the potential consequences of human exposure to industrial-scale carbon black (CB) particles, but limited human toxicological data is currently available. The production of CB consists of a three-step process: reaction, pelletizing, and packaging (Kuhlbusch et al. 2004). In the reaction step, chemical reactions take place in a furnace reactor to produce the primary CB particles with particle sizes ranging from 1 to 500 nm, where the most common particles are in the range of 10 to 100 nm range. In the pelletizing step, large agglomerates (pellets) are formed by tumbling the newly made CB in a drum by mixing with water.

In the packaging step, workers pack the agglomerated CB pallet particles in 25-kg or 1000-kg bags for shipping. Here, the occupational workers are most susceptible to exposure by coming in close contact with inhalable particles, where the average mass concentration of PM with a dae from 100 nm to 1000 nm is on the order of 240 $\mu g.m^{-3}$, which is twenty times more concentrated than that of comparable but safe ambient sites (Kuhlbusch et al. 2004). The in vivo study at a CB production plant in Beijing, China, conducted by Zhang et al. (2014), showed that the CB particles are partially responsible for altered lung function and inflammation of packaging workers exposed to acetylene CB particles. Their comparison sites maintained a PM level according to the guidelines recommended by the American Conference of Governmental Industrial Hygienists, the American Industrial Hygiene Association, and the German MAK Commission (Brook et al. 2004).

Exposure to UFPs in the metal industry workplaces is also a health concern to occupational workers, causing an increased risk of developing respiratory, cardiovascular, and neurological disorders. Wire-cut electrical discharge machining (WEDM) is very popular in die and mold manufacturing industries for producing delicate concave shape products. This process utilizes a high voltage between the wire electrode and the conductive metal pieces to cause flamboyant energy sparks, which remove material by melting and erosion, and the high-energy electrophysical process is the primary cause for generating nano-sized iron oxide particles (Tonshoff et al. 1996, Sivapirakasam et al. 2011). In a typical WEDM machine shop, nanoparticle number concentration is dominated by particles with $d_{ae} \leq 30$ nm, while particles with dae ≥ 60 nm dominate mass and surface area concentration.

Tian et al. (2017) reported an in vitro inhalation study with realistic nasal and upper airway replicas and extrapolated the human lung tumor risk recommended exposure limits of WEDM-generated UFPs mass and number concentrations. However, their study could not show the effects of particle size distribution on deposition fraction or the implication to the human lung's regional airway in vivo dosages because such studies have health risks involved. Moreover, the investigations on detailed human inhalation and PM transport processes are restrictive from time, cost, and ethical perspectives. Also, in view of the health risks involved, individuals cannot be exposed to various toxic UFPs under different breathing scenarios and working conditions (Hofmann 2011, Nahar et al. 2013). Besides, these toxicities are inherent in the industrial workplace's ambient air.

To overcome this problem, in silico modeling and simulation can be an alternative way to computationally replicate the particle flow, distribution, and deposition. Understanding these limitations and opportunities, the present work adopted the Multiple Path Particle Dosimetry (MPPD) model based on a stochastic human lung morphology with realistic asymmetries at the airway branching structure. The novelty of this work is that the MPPD modeling technique closely fits reality due to its application of actual airway geometry (e.g., diameter, length, trachea-bifurcation angle, and intrabronchial angles) and the asymmetry of lung morphology (Bui et al. 2020). Moreover, the deposited PM concentration in each airway is calculated as a function of time for the proximal and distal ends.

There were two objectives of this work. Compare and fit MPPD model simulated data of the total lung deposition, regional deposition, and deposited mass of particles in regard to time and size distributions with (1) in vivo data on CB particles exposed workers' pulmonary function and pro-inflammatory cytokines conducted by Zhang et al. (2014) and (2) lung burden data of in vitro WEDM particles deposition investigation by Tian et al. (2017).

MATERIALS AND METHODS

The present in silico study employed the MPPD simulation model computer software version 3.04, developed by Applied Research Associates (ARA) of Albuquerque, New Mexico, USA (ARA 2021). The MPPD is a software accepted by the inhalation toxicology scientific community. This computational model can estimate human and laboratory animal inhalation particle dosimetry. The model applies to risk assessment, research, and education, as reported elsewhere (Miller et al. 2016, Li et al. 2016, Backman et al. 2018, Manojkumar et al. 2019, Kuprat et al. 2021).

There have been confirmed cases and reports demonstrating the link between human pulmonary functional impairment and chronic exposure to various doses of metallic particles (Mayer-Baron et al. 2007, Nahar et al. 2013). In the MPPD simulation model, mechanistic modeling of local exposure can potentially speed up and improve the chances of successfully estimating inhaled particles. This multiscale computer model was designed to reasonably predict regional depositions of fine and UFP exposure following inhalation. Furthermore, these computer-based models are useful for comparing the available underpinning in vivo and in vitro data. Here, the physical, mechanical, and electrical properties of CB-PMs with a size range of 100 nm $\leq d_{ae} \leq$ 1000 nm and UFPs from WEDM, with mass median d_{ae} in the range of 1 to 100 nm, were used as input parameters of the MPPD.

A flowchart of the Multiple Path Particle Dosimetry simulation sequence and implementation is given in Fig. 1. The model can run single or batch jobs with age-specific lung geometries, and plots can be drawn for mass flux or mass per surface area vs. lung generations or anatomical units. The MPPD user chooses various parameters of airway morphometry, inhalant properties, exposure boundary conditions, deposition, and clearance. The setting loop continues until the user accepts upon reviewing the simulation protocol.

In vitro experimental study indicated that the quantity of particles reaching the respiratory tract is directly proportional to the lung burden. However, the particle deposition in the lungs is also governed by other factors. For example, the diameter of the inhaled particles, the concentration of

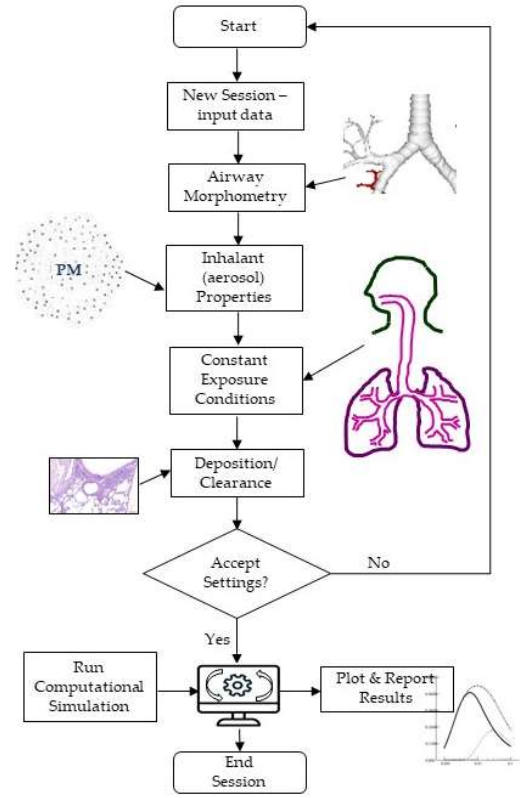

Fig. 1: The flowchart of the Multiple Path Particle Dosimetry simulation sequence and implementation.

particles per unit volume, and the inhalation rate constitute the determinant factors for their deposition in different parts of the respiratory tract (Yeh et al. 1976). This deposit interacts with different fundamental physical, aerodynamic, and electromechanical mechanisms. Among them, the inertial impaction, gravitational settling, Brownian diffusion, and the electrostatics forces are dominant processes (Ali et al. 2009, Hinds 2012). Asgharian et al. (2001) listed the original studies during the past six decades that were undertaken to develop the fundamental mathematical equations of these deposition mechanisms, and the MPPD computational model implemented these calculations in its software coding. Additional information on the MPPD model development and its features can be found elsewhere (Miller et al. 2016).

In the MPPD model, PM deposition computations are available for twenty-eight human respiratory airway anatomical units (Asgharian et al. 2001, Kuprat et al. 2021). Each anatomical unit is called a generation. Nevertheless, it is typical in most respiratory deposition studies to include twenty-four generations by counting the trachea as the first generation and the alveolar sacs as the last generation. Prior to the trachea, the MPPD considers four anatomical units, including the nose, mouth, esophagus, and larynx,

as the Head region. Thereafter, it considers the trachea to an additional fifteen anatomical units up to the terminal bronchioles as the tracheobronchial (TB) region and from the respiratory bronchioles to the alveolar sacs as the pulmonary (P) region.

The MPPD simulation assumes an average lung morphometry for the study population. There may be interindividual variability in airway structure, which may cause variations with in vitro studies. It also considered airway branching to be perfectly dichotomous. Furthermore, each airway branch is assumed to be cylindrical and straight, characterized by length, diameter, the angle the airway makes with its parent, and a gravity angle.

The model calculated the deposition fraction (DF) as the ratio of specific-size particles deposited in a particular region (Head, TB, and P) to the number of same-size particles entering the region. This notion is aligned with the reported literature (Cheng 1995). The PM, properties such as density, aspect ratio, diameter, or size, are necessary for calculation. In this model, the diameter can be specified to any of the three choices: count median diameter, mass median diameter, or mass median aerodynamic diameter. The DF can be estimated and visualized at simulation outputs for particles between 1 nm and 100 μm. The model offers morphometry of several species, such as humans, rhesus monkeys, rats, mice, pigs, and rabbits. Here, the human species was selected. The MPPD incorporated a stochastic model with asymmetries, representing the sixtieth percentile of lung-size population for Chinese adult airways to fit study objectives. Such airway branching structure provides more realistic flow and transport, eventually minimizing errors in deposition predictions.

To run the simulation software, input data such as airway morphometry, exposure conditions, and PM properties must be provided by default or user-specified values. Workers' lung airway morphometric parameters were as follows: gender was male, average age was forty-five years, BMI was 25 $kg.m^{-2}$, and the body was in an upright orientation while working. The user-specified values were given for the functional residual capacity (3174 mL), upper respiratory tract volume (50 mL), breathing frequency (16), and tidal volume (537.5 mL) to comply with the International Commission on Radiological Protection (ICRP) and model recommendations (ICRP 1994).

The fine or ultrafine particles generated from CB and WEDM are usually of irregular shapes, so the equivalent d_{ae} was necessary to determine by the in situ scanning mobility particle spectrometer, as reported in both studies. These input data were applied in the MPPD to quantify the number and mass depositions of particles in the human airway, including the Head or extrathoracic, TB, and P regions of the exposed workers in the industrial workplace. PM size data was converted into mass data using the formula mass = density × volume. The mass, m, of each particle, was therefore calculated by the following equation:

$$m = \frac{\rho \pi d_{ae}^3}{6} \quad ...(1)$$

P is the unit density, and d_{ae} is the aerodynamic diameter or particle size. The MPPD calculates particle size distribution data, which can be analyzed by an Excel spreadsheet and develop the necessary plots. The model was developed for assessing deposition and clearance doses upon specifying all the input data.

RESULTS AND DISCUSSION

Currently, too few examples in the literature combine a transparent presentation of key in vivo or in vitro UFPs as lung dosages. Therefore, epidemiological outcomes and mechanistic in silico model simulations are warranted to provide a sufficient database for validating and improving existing mathematical models. From this point of view, the adopted MPPD computational model in the present study provides necessary transparency regarding underlying assumptions, which may open the accessibility and acceptance by peer reviewers. Here, the simulation methodologies followed the same approaches as previously reported literature (Miller et al. 2016, Li et al. 2016, Backman et al. 2018, Manojkumar et al. 2019, Kuprat et al. 2021).

Fit with Known Data of Zhang et al. (2014)

In their in vivo study on toxicological data of CB particles in the workplace, Zhang et al. (2014) found evidence of a link between human exposure to acetylene CB and long-term pulmonary effects. Their study focused on a work environment of CB production's packaging facility, where 51% of particles were less than 523 nm ($d_{ae} < 0.523$ μm), and the remaining were in the size range of 523 nm to 1000 nm. The mean particle concertation was 14.9 mg/m^3, 4.26 times higher than the NIOSH suggested threshold of 3.5 $mg.m^{-3}$ (Cassinelli and O'Connor 1994). The study subjects were 81 human volunteers with an average age of forty-five years at a CB production plant in Beijing, China, and the control was 104 nonexposed male workers.

In the experimental protocol, Zhang et al. (2014) evaluated clinical symptoms and lung functions of forced expiratory volume in 1 second (FEV1%), percent predicted peak expiratory flow (PEF%), and percent predicted maximal mid-expiratory flow (MMF%). These indicators were 5.54, 15.26, and 9.79 percent decrease compared with

the control workers. The pro-inflammatory cytokine levels in the serum of CB-exposed workers were 2.86 to 4.87 fold higher compared to controls. In summary, their study evidenced a link between human exposure to CB and lung functional impairments, which led to the toxicity of long-term respiratory distress.

To fit with the in vivo study, the present in silico MPPD modeling simulated CB exposure standard particle size distribution from 100 nm (0.1 μm) to 1000 nm (1 μm) and other PM properties as reported by Zhang et al. (2014). Also, their study subjects were male workers with an average age of forty-five years and an average BMI of 25 $kg.m^{-2}$. These values are considered as inputs of the MPPD's human physiological parameters. In addition, the PM exposure parameters include upright body orientation, 16 oronasal (nose and mouth combined) breathing frequency per minute, and 537.5 ml of tidal volume, as Roy et al. (1991) suggested. The breathing scenario was chosen as oronasal, a combination of nose and mouth breathing. The inspiratory fraction and tracheal mucous velocity were chosen to be 0.5 and 5.5 mm/min, respectively, to comply with ICRP and model recommendations.

The model also used the deposition and clearance approach because occupational workers usually breathe in this mode (Niinimaa et al. 1981). In a typical working day, a worker experiences a constant exposure of about six hours per shift except for lunch and other breaks. As such, each worker was assumed to be exposed for a period of six h/day, five days/week, and forty-four weeks/year. The model calculated lung deposition during exposure by the amount deposited in one breathing cycle.

The MPPD simulating human lungs' first ten generations of TB region is shown in Fig. 2. Even though the PM deposition calculation was done for all twenty-eight generations, Fig. 2 does not include respiratory bronchiole and P regions purposely because the entire lung geometry artifact will become an image of a black sponge where airway splitting will be invisible.

Fig. 2: Simulated lung geometry 1-10 airway generations or lung's anatomical units.

Notably, empirical and typical-path lung models are useful when quick calculations of regional and overall PM depositions are sought, but they produce limited information. Therefore, multiple-path and stochastic models are adopted in this study to determine more detailed site-specific deposition information like other computational fluid dynamics modeling techniques adopted by Kolanjiyila &Kleinstreuer (2017).

The conventional PM dosimetry recommendations are particles' either number or mass concentrations within a fixed aerodynamic size. So, as the present MPPD simulation model calculated both deposition and clearance of CB industrial workplace PM pollutants, Fig. 3 illustrates the particle size distributions deposited in various lung regions. Here, the total lung dose of 100 nm particles is the highest (28%), while 380 nm size particles are the lowest (15%). After that, the deposition increases with particle size again and reaches 26% for 1000 nm (1.0 μm). The size-segregated DF count of all inhaled particles is 20% in the entire respiratory airway of the lung. Out of these particles, about 27% are deposited in the Head airways. From the remaining 73% of particles, 32% and 41% deposit in the TB and P regions, respectively (Fig. 3).

The computed results demonstrated that the CB-PMs deposit highly in the TB and P regions. There is an important phenomenon that we will be going to explain here. As mentioned in the Introduction section, most CB particles leave the reactor in the 10 to 100 nm size range. Subsequently, large agglomerates (pellets) are formed by tumbling the newly made CB in a drum by mixing with water at the pelletizing step.

Moreover, Zhang et al. (2014) reported that these finished product particles with a 523 nm to 1000 nm size go for packaging, the last step of CB production. These particles

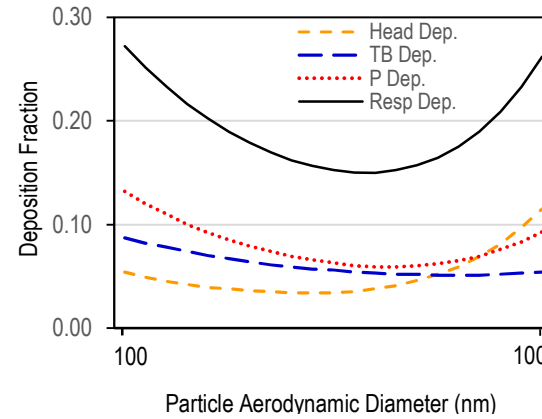

Fig. 3: Respiratory regional deposition fraction of inhaled carbon black PMs w.r.t particle size distribution. TB: tracheobronchial, P: pulmonary, Dep: deposition.

are heavier and neutral or carry no electrostatic charges. So, they tend to follow the inhaled fluid flow smoothly and move into the deeper lung to experience higher gravitational sedimentation and deposit superbly during each breath's pause moment.

Assessment of the total deposition of size-segregated PM fraction in the entire human lung airway is essential for further regional deposition investigations. The simulation model analysis showed that the total PM mass and count deposition in the human respiratory airways were 49% and 56% for 523 nm and smaller particles, respectively. Fine particles exhibited a higher mass deposition fraction (48%) in the Head and significantly (33%) in the P regions. Similar patterns are confirmed by the MPPD-generated images of deposited CB-PM mass at various lung lobes and mass flux per min (see Fig. 4a and 4b).

Fig. 4a shows the simulated visualizations of deposited CB-PM mass in the Head, TB, and P regions. It is found that PM mass concentration could reach as much as up to $2.23x10^{-2}$ µg at the distal airways and the alveolar sacs. Fig. 4b depicts the simulated visualizations of deposited PM mass flux rate per unit area from the Head, TB, to P airways. It is also observed that the PM mass deposition rate could reach up to $2.72x10^{2}$ µg/min/m^2. Observations in terms of DF in the line graphs confirm this trend.

To summarize, the in vivo study results of Zhang et al. (2014) and the present in silico MPPD simulations confirmed a relationship between CB-PMs as exposed in the workplace environment and altered lung functions of CB workers. However, it is difficult to further study the deposition characteristics using lung dissections following CB inhalation and the follow-up changes of lung inflammation in CB-exposed workers. Animal inhalation experiments could be pursued to mimic the exposure conditions of CB workers.

Fit with Known Data of Tian et al. (2017)

To determine the toxicity from exposure to UFPs in the WEDM process shop in Beijing, China, Tian et al. (2017) conducted an in vitro study. The UFPs were characterized in real-time at the production site, and this study found substantial emission of nano-pollutants by WEDM processes. The particle mass concentration was 27 mg/m^3, and the size distribution was in the range from 5.52 nm to 98.2 nm during a typical working day. Based on experimental data, the study found that particle dosimetry was extremely sensitive to real-time particle concentration and size distribution. To complement in vitro data, Tian et al. (2017) also carried out human inhalation simulations with realistic exposure conditions in a physiologically mimicked nasal and upper airway replica. Both study methodologies detected a substantial enhancement of WEDM respiratory DF with respect to UFP's number, mass, and surface area properties. For instance, study subjects' lungs acquired up to thirty-three-fold in mass, twenty-seven-fold in surface area, and eight-fold in number of dosages during working hours compared to controls.

A typical working day in the WEDM shop is from 8:00 a.m. to 5:30 p.m. The UFPs' exposure time is assumed to be 8 h, leaving 1.5 h for lunch and other activities. Mild physical activity was assumed because the machine operators perform their job responsibilities by mainly standing with the occasional walking to attend to the metal pieces. To fit with the in vitro study, the present in silico MPPD modeling simulated WEDM exposure standard particle size distribution from 1 nm to 100 nm and other UFP properties, as reported

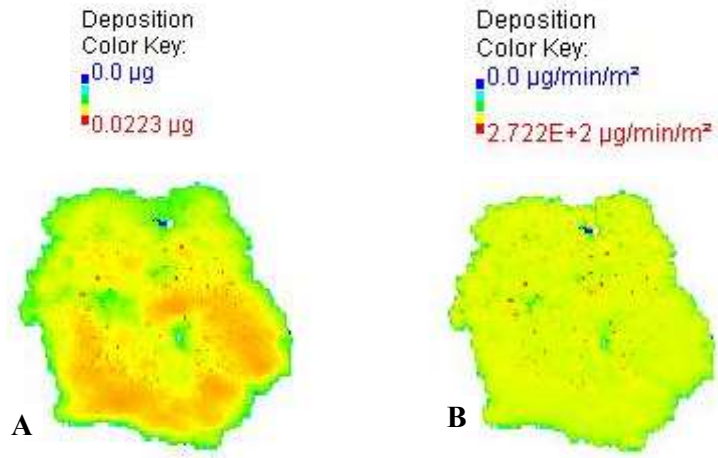

Fig. 4: Visualization of deposited CB-PMs at various lung lobes: (a) total mass; (b) mass flux per min per unit rate.

by Tian et al. (2017). In addition, it mimicked occupational workers' light breathing (12 $L.min^{-1}$) oronasal, a combination of nose and mouth breathing exposure. Here, it is notable that particle number counts are high for smaller particles, d_{ae} < 20 nm, but their mass concentration is negligible. The mass concentration for larger than this size monotonically increases with particle size.

The MPPD model's human physiological parameters were employed, including an age of forty-five years and a BMI of 25 $kg.m^{-2}$. Moreover, the PM exposure parameters include upright body orientation, 16 oronasal (nose and mouth combined) positions, a breathing frequency per minute of 537.5 ml of tidal volume, and a pause and inspiratory fraction of 0.5, as Roy et al. (1991) suggested. The model also used a deposition and clearance approach because occupational workers usually breathe in this mode (Niinimaa et al. 1981). The typical constant exposure times at the WEDM packaging area are six hours per shift, five days a week, and forty-four weeks per year. Finally, the model output recommendations are in the total mass in number concentrations format. The MPPD model's human physiological parameters include an age of forty-five years and a BMI of 25 $kg.m^{-2}$. Fig. 5 illustrates the respiratory DF of inhaled WEDM UFPs with respect to the particle size distribution. In this simulation, inhaled UFP aerosol mass concentration and density were 27 $mg.m^{-3}$ and 2.7 $g.cm^{-3}$, respectively. Out of all deposited PMs, 50% of particle counts had an aerodynamic diameter of 5 nm or less. No particles smaller than 5 nm could reach the pulmonary region. The simulation also shows that 86% of all inhaled UFPs were deposited in the Head (mouth-throat) and tracheobronchial regions.

The present simulation calculated both deposition and clearance of WEDM industrial workplace UFP pollutants. The size-segregated DF count of all inhaled particles is 75% in the entire respiratory airway of the lung. Out of all deposited particles, about 44% settled in the Head airways. From the remaining 56% of particles, 38% and 18% were deposited in the TB and P regions, respectively (Fig. 5). The UFP tends to deposit highly in the Head and TB regions. Each particle's diffusive bombardment while wiggling in the lung's tabular airway can better explain this phenomenon. In addition, their Coulombic attraction (opposite charges between particles), due to electrostatic space charge force, and repulsion, due to same-charge polarity induced image charge forces, caused them to move toward the conductive airway walls and deposit subsequently.

In practice, the smaller the particle, the higher the charge-to-mass ratio and surface area. Therefore, the highest number of particles deposited in the Head region was smaller than 6.5 nm. In contrast, particles within the 25 to 35 nm size tend to deposit in the P region. This situation can be explained. As these particles pass conducting airways, they may lose charge by acquiring moisture from lung airways and become heavier and susceptible to deposit by gravitational sedimentation. Deposited mass per area in the lung's periphery or pulmonary regions is negligible for WEDM UFPs. See similar observations in the deposition line graphs of Fig. 6.

Tian et al. (2017) used industry-standard micro-nano-particle sizing, counting, and mobility analyzer instruments in their study. Their particle spectrometry detected 104/cc counts centration, which construed a mixture of iron, aluminum, copper, and trace elements of Mg, Mn, Mo, Zn, Ni, and Cr. These metallic components create larger (about

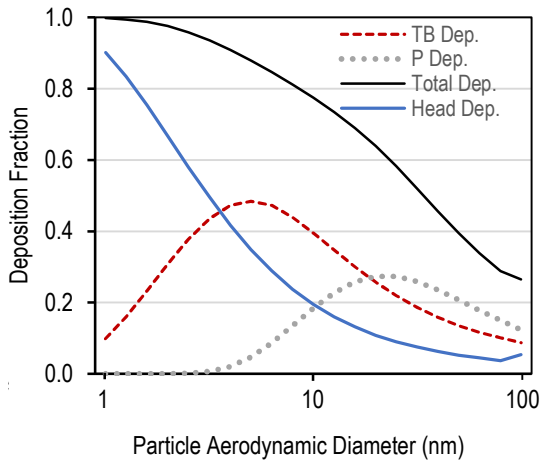

Fig. 5: Respiratory regional deposition fraction of inhaled wire-cut electrical discharge machining UFPs w.r.t particle size distribution. TB: tracheobronchial, P: pulmonary, Dep: deposition.

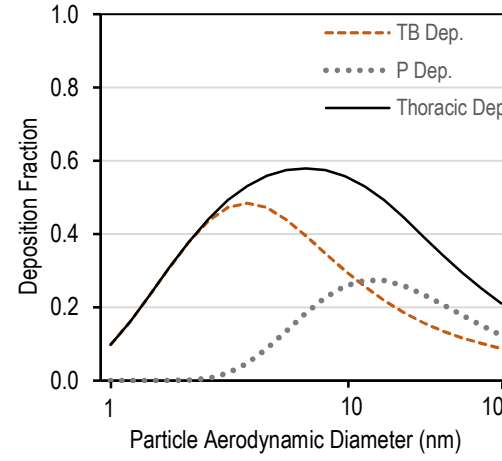

Fig. 6: Thoracic deposition fraction of inhaled wire-cut electrical discharge machining UFPs w.r.t particle size distribution. TB: tracheobronchial, P: pulmonary, Dep: deposition.

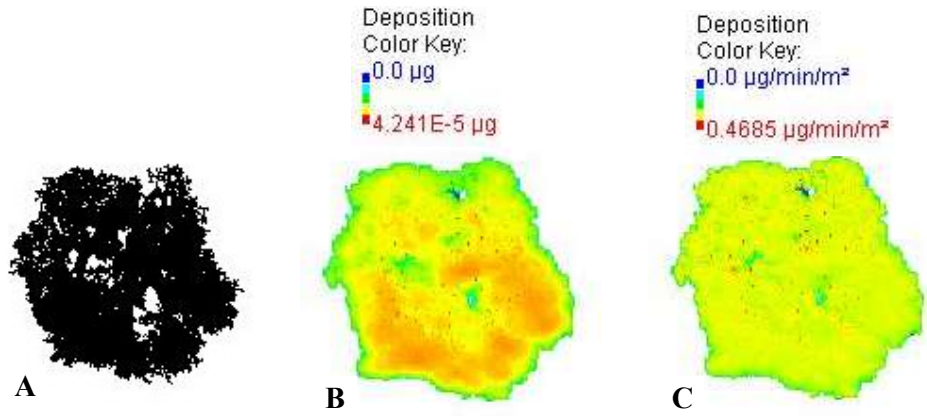

Fig. 7: Visualization of simulated lung geometry and deposited WEDM-UFPs at various lung lobes: (a) Stochastic lung morphological structure up to 16 generations; (b) Total mass deposition; (c) Mass flux per min per unit rate at various lobes.

2700 kg.m^{-3}) particle density. The MPPD used this value and calculated mass a deposition rate in 29.3 µg.m^{-2}.

Fig. 7a shows the simulated lung geometry or morphological structure up to sixteen generations. The remaining distal airways, including alveolar sacs, are not intentionally shown to prevent the image from becoming full solid black. Fig. 7b depicts the simulated visualizations of deposited UFP mass in the Head, TB, and P regions. It is found that the PM mass concentration could reach as much as up to 4.24 x 10^{-5} µg at the distal airways and alveolar sacs.

Fig. 7c depicts the simulated visualizations of deposited UFPs mass flux rate per unit area from the Head, TB, to P airways. It is found that PM mass flux concentration could reach as much as up to 0.47 µg.min^{-1}.m^{-2}. Deposited mass per area in the lung's periphery or pulmonary regions is negligible for WEDM UFPs. See similar observations of depositions in line graphs in Fig. 5. This phenomenon can be explained by the fact that particles smaller than 50 nm experience higher surface charge-to-mass ratio, which caused them to deposit at the conductive Head and TB airways due to both space and image charge forces (Dumitran et al. 2008) because the particles' charge distributions are governed by their size and dielectric properties (Ali 2021, 2022).

All these studies have a good relationship with our present study results. Yet, our study's variation in deposition percentage is mainly due to the airway geometry, PM size, and unconsidered deposition mechanisms such as interception, van der Waals force, and adhesive force due to their negligible effects. More eminently, the MPPD mathematical equations considered all four crucial mechanisms that influence the PM depositions in airways, including (1) initial impaction, (2) gravitational sedimentation, (3) Brownian diffusion, and (4) electrostatic image/space charge forces.

Computational modeling and simulations can predict the UFP burden in the workers' lungs. However, the definitive evaluation of CB-induced carcinogenic effects is still insufficient, and more evidence from epidemiological studies in humans will help to understand the adverse effects of CB. Comparison of reported data (Zhang et al. 2014, Tian et al. 2017) versus model-predicted lung burdens in human lungs shows that the MPPD predictions are reasonably good. The simulated retained mass of poorly soluble fine and ultrafine particles in humans exposed to chronic inhalation occurs. To our knowledge, there is limited in vivo experimental data on regional-level deposition for CB- or WEDM-PM aerosols in human lungs.

Future work on additional model validation is needed for fine or ultrafine PMs of varying chemical characteristics. Such analyses would improve these particle doses' prediction for occupational safety and risk assessment.

Study Limitations

The computer-based models lack direct clinical validation beyond the first few airways (oropharynx and trachea) of the human lung's large conducting regions since available imaging methods (e.g., gamma scintigraphy) lack the required resolution (Backman et al. 2018). This drawback limits the full evaluation of deposition model robustness. Nevertheless, successful development and application of any pharmacokinetic modeling and simulation to predict regional exposure is likely to require at least an assessment of lung dose and, optimally, an assessment of deposition pattern, for example, distribution of particles in the lungs.

CONCLUSIONS

The present computational model has demonstrated the predictive power as a supplement to physical (either in

vivo or in vitro) models for assessing fine and ultrafine PM deposition in the realistic airways of extrathoracic, tracheobronchial tree, and pulmonary alveolar sacs like other models.

Compared with one in vivo and one in vitro source of experimental data in this work, satisfactory agreements are found regarding toxicity burdens and pulmonary function reduction. For example, a total lung dose of 100 nm CB-PMs is the highest (28%), while 380 nm is the lowest (15%). Afterward, deposition increases with particle size, reaching 26% for 1000 nm.

In the case of WEDM-UFPs, about 98% of all 1.0 nm inhaled particles remain in the lung. Subsequently, the deposition dose decreases with the particle size, reaching up to 28% for 100 nm size. Another notable point is that approximately 51% of deposited WEDM-UFPs are of CMAD $\leq$ 5 nm. Maximum deposited mass and mass flux rate in the Head, tracheobronchial, and pulmonary airways were also examined by the images of lung geometry.

Computational simulation of lung doses of harmful UFPs can overcome risks associated with investigations on detailed human inhalation, particle flow, and transport processes, which are restrictive from time, cost, and ethical perspectives. In conclusion, the practical application of this work demonstrated that the successful application of transparent mechanistic in silico models accompanied by robust experimental data on toxicity mechanisms could benefit the discovery of UFP inhalation toxicity to workers in chemical, steel, cement, and other industrial workplaces.

ACKNOWLEDGMENTS

This work was supported in part by the Office of Research and Scholarship at the University of Texas at Tyler, USA. The author acknowledges Applied Research Associates of Albuquerque, New Mexico, USA, for granting the use of MPPD simulation model computer software.

REFERENCES

Abraham, J.L., Hunt, A. and Burnett, B.R. 2002. Quantification of non-fibrous and fibrous particulates in human lungs: twenty-year update on pneumoconiosis database. Ann. Occup. Hyg., 46(1): 397-401.

Ali, M. 2014. Engineered aerosol medicine and drug delivery methods for optimal respiratory therapy. J. Respir. Care, 59(10): 1608-1610. https://doi.org/10.4187/respcare.03634.

Ali, M. 2021. Computational fluid dynamics simulation of inhaled submicron bioaerosol particles flow and deposition in the human lung. Intl. J. Modern Engrg., 22(1): 5-11.

Ali, M. 2022. Multiple path particle dosimetry modeling employability to complement in-vitro ultrafine particle toxicity study. Current Trends Engrg. Sci., 2(2). DOI: 10.54026/CTES/1017.

Ali, M., Mazumder, M. K. and Martonen, T. B. 2009. Measurements of electrodynamic effects on the deposition of MDI and DPI aerosols in a replica cast of human oral-pharyngeal-laryngeal airways. J. Aerosol Med. Pulmon. Drug Del., 22(1): 35-44. https://doi.org/10.1089/jamp.2007.0637.

ARA (Applied Research Associates) 2021. Multiple Path Particle Dosimetry Model Version 3.04 [Computer Software]. Retrieved from https://www.ara.com/mppd. Retrieved 19 September 2021.

Asgharian, B., Hofmann, W. and Bergman, R. 2001. Particle deposition in a multiple-path model of the human lung. Aerosol Sci. Techno., 34(4): 332-339.

Backman, P., Arora, S. Couet, W., Forbes, B., Kruijf, W. and Paudel, A. 2018. Advances in experimental and mechanistic computational models to understand pulmonary exposure to inhaled particles. European J. Pharma. Sci., 113: 41-52. https://doi.org/10.1016/j.ejps.2017.10.030

Brook, R.D., Franklin, B., Cascio, W.E., Hong, Y., Howard, G., Lipsett, M., Luepker, R.V., Mittleman, M.A., Samet, J.M., Smith, S.C.J. and Tager, I.B. 2004. Air pollution and cardiovascular disease: A statement of the health care professionals from the expert panel on population and prevention science of the American Heart Association. Circulation, 109: 2655-2671.

Bui, V.K.H., Moon, J.Y., Chae, M., Park, D. and Lee, Y.C. 2020. Prediction of aerosol deposition in the human respiratory tract via computational models: a review with recent updates. Atmosphere, 11: 137-163. https://doi:10.3390/atmos11020137.

Cassinelli, M.E. and O'Connor, P.F. 1994. NIOSH manual of analytical methods. National Institute for Occupational Safety and Health. http://niosh.dnacih.com/nioshdbs/nmam/pdfs/5000.pdf. Retrieved 24 September 2021.

Cheng, K., Swift, D. L., Cheng, K. and Swift, D. L. 1995. Calculation of total deposition fraction of ultrafine aerosols in human extrathoracic and intrathoracic regions calculation of total deposition fraction of ultrafine aerosols in human extrathoracic and intrathoracic regions. Aerosol Sci. Technol., 22: 194-201. https://doi.org/10.1080/02786829509508887.

Ding, Y., Kuhlbusch, T.A.J., Tongeren, M. V., Jiménez, A. S., Tuinman, I., Chen, R. Alvarez, I.L., Mikolajczyk, U., Nickel, C., Meyer, J. Kaminski, H., Wohlleben, W., Stahlmecke, B., Clavaguera, S. and Riediker, M. 2017. Airborne engineered nanomaterials in the workplace- A review of release and worker exposure during nanomaterial production and handling processes. J. Hazard. Mater., 322: 17-28.

Douafera, H., Andrieub, V. and Brunela, J.M. 2020. Scope and limitations on aerosol drug delivery for the treatment of infectious respiratory diseases. J. Contr. Rel., 325: 276-292. https://doi.org/10.1016/j.jconrel.2020.07.002.

Dumitran, L.M., Blejan, O., Notingher, P., Samuila, A. and Dascalescu, L. 2008. Particle charging in combined corona-electrostatic fields. IEEE Trans. Ind. Appl., 44(5): 1385-1390. https://doi.org/10.1109/TIA.2008.2002935.

Hinds, W.C. 2012. Aerosol Technology: Properties, Behavior and Measurement of Airborne Particles. Second Edition. Wiley, New York.

Hofmann, W. 2011. Modelling inhaled particle deposition in the human lung: A review. J. Aerosol Sci., 4(10): 693-724. doi:10.1016/j.jaerosci.2011.05.007.

ICRP. 1994. Human Respiratory Tract Model or Radiological Protection. ICRP Publication 66. Ann. ICRP, 1-3. https://www.icrp.org/publication.asp?id=icrp%20publication%2066. Retrieved 24 September 2021.

Kolanjiyila, A.V. and Kleinstreuer, C. 2017. Computational analysis of aerosol dynamics in a human whole-lung airway model. J. Aerosol Sci., 114: 301-316. https://doi.org/10.1016/j.jaerosci.2017.10.001.

Kuhlbusch, T.A.J., Neumann, S. and Fissan, H. 2004. Number size distribution, mass concentration, and particle composition of PM1, PM2.5, and PM10 in bag-filling areas of carbon black production. J. Occup. Envir. Hygiene, 1(10): 660-671. DOI: 10.1080/15459620490502242

Kuprat, A.P., Jalali, M., Jan, T., Corley, R.A., Asgharian, B., Price, O., Singh, R.K., Colby, S. and Darquenne, C. 2021. Efficient bi-directional

coupling of 3D computational fluid-particle dynamics and 1D Multiple Path Particle Dosimetry lung models for multiscale modeling of aerosol dosimetry. J. Aerosol Sci., 151, https://doi.org/10.1016/j.jaerosci.2020.105647.

Li, X., Yan, C., Patterson, R.F., Zhu, Y., Yao, X., Zhu, Y., Ma, S., Qiu, X., Zhu, T. and Zheng, M. 2016. Modeled deposition of fine particles in the human airway in Beijing, China. Atmos. Environ., 124: 387-395. http://doi.org/10.1016/j.atmosenv.2015.06.045

Manojkumar, N., Srimuruganandama, B. and Nagendrab, S.M.S. 2019. Application of multiple-path particle dosimetry model for quantifying age-specified deposition of particulate matter in the human airway. Ecotoxicol. Environ. Safety, 168: 241-248. https://doi.org/10.1016/j.ecoenv.2018.10.091.

Matsoukas, T., Desai, T.G. and Lee, K. 2015. Engineered nanoparticles and their applications. J. Nanomatls, 2: 1-2. doi:10.1155/2015/651273.

Meyer-Baron, M., Schaper, M., Knapp, G. and Thriel, C.V. 2007. Occupational aluminum exposure: evidence in support of its neurobehavioral impact. Neurotoxicology, 28: 1068-1078.

Miller, F.J., Asgharian, B., Schroeter, J.D. and Price, O.T. 2016. Improvements and additions to the Multiple Path Particle Dosimetry model. J. Aerosol Sci., 99: 14-26.

Nahar, K., Gupta, N., Gauvin, R., Absar, S., Patel, B., Gupta, V., Khademhosseini, A. and Ahsan, F. 2013. In vitro, in vivo, and ex vivo models for studying particle deposition and drug absorption of inhaled pharmaceuticals. Euro. J. Pharma. Sci., 49: 805-818. https://doi.org/10.1016/j.ejps.2013.06.004.

Niinimaa, V., Cole, P. and Shephard, R.J. 1981. Oronasal distribution of respiratory airflow. Respir. Physiol., 43(1): 69-75. https://doi.org/10.1016/0034-5687(81)90089-X.

Roy, M., Becquemin, M.H. and Bouchikhi, A. 1991. Ventilation rates and lung volumes for lung modeling purposes in ethnic groups. Rad. Protect. Dosimet., 38(1-3): 49-55. https://doi.org/10.1093/rpd/38.1-3.49.

Seong Jo, M,. Kim, J.K., Kim, Y., Kim, H.P., Kim, H.S., Ahn, K., Lee, J.H., Faustman, E.M. Gulumian, M., Kelman, B. and Yu, J. 2020. Mode of silver clearance following 28-day inhalation exposure to silver nanoparticles determined from lung burden assessment, including post-exposure observation periods. Arc. Toxicol., 94: 773-784. https://doi.org/10.1007/s00204-020-02660-2

Sivapirakasam, S.P., Mathew, J. and Surianarayanan, M. 2011. Constituent analysis of aerosol generated from die sinking electrical discharge machining process. Process Safety Environ. Protec., 89(2): 141–50.

Tian, L., Shang, Y., Chen, R., Bai, R., Chen, C., Inthavong, K. and Tu, J. 2017. A combined experimental and numerical study on upper airway dosimetry of inhaled nanoparticles from an electrical discharge machine shop. Particle Fibre Toxicol., 14, Article 24. DOI 10.1186/s12989-017-0203-7.

Tonshoff, H.K., Egger, R. and Klocke, F. 1996. Environmental and safety aspects of electrophysical and electrochemical processes. CIRP J. Manufac. Sci. Techno., 45(2): 553-68.

Yeh, H.C., Phalen, R.F. and Raabe, G. 1976. Factors influencing the deposition of inhaled Particles. Environ. Health Perspect., 15: 147-156.

Zhang, R., Dai, Y., Zhang, X., Niu, Y., Meng, T., Li, Y., Duan, H., Bin, P., Ye, M., Jia, X., Shen, M., Yu, S., Yang, X., Gao, W. and Zheng, Y. 2014. Reduced pulmonary function and increased pro-inflammatory cytokines in nanoscale carbon black-exposed workers. Particle Fibre Toxicol., 11: 73. DOI 10.1186/s12989-014-0073.

ORCID DETAILS OF THE AUTHORS

M. Ali: https://orcid.org/0000-0001-7255-5038